Confined Brownian motion of individual magnetic nanoparticles on a chip: Characterization of magnetic susceptibility.

Confined Brownian motion of individual magnetic nanoparticles on a chip: Characterization of magnetic susceptibility

Kim van Ommering[a] and Jeroen H. Nieuwenhuis
Philips Research Laboratories, 5656 AE Eindhoven, The Netherlands

Leo J. van IJzendoorn and Bert Koopmans
Department of Applied Physics, Eindhoven University of Technology, 5600 MB Eindhoven, The Netherlands

Menno W. J. Prins
Philips Research Laboratories, 5656 AE Eindhoven, The Netherlands and Department of Applied Physics, Eindhoven University of Technology, 5600 MB Eindhoven, The Netherlands

(Received 5 May 2006; accepted 21 August 2006; published online 6 October 2006)

An increasing number of biomedical applications requires detailed knowledge of the magnetic susceptibility of individual particles. With conventional techniques it is very difficult to analyze individual particles smaller than 1 μm. The authors demonstrate how the susceptibility of individual nanoparticles can be determined in an efficient way by optically analyzing the confined Brownian motion of a nanoparticle trapped in a known magnetic potential well on a chip. A setup is introduced that has a controllable two-dimensional magnetic potential well, which is defined by an integrated microscopic current wire. Susceptibility measurements have been performed on 150–450 nm superparamagnetic beads. They found differences in bead susceptibility of an order of magnitude and differences in volumetric susceptibility of more than a factor of 2. © *2006 American Institute of Physics*. [DOI: 10.1063/1.2360246]

Magnetic particles are very important in the field of biomedical applications, such as for magnetic extraction of biological material and for use as contrast agents in magnetic resonance therapy.[1] These techniques do not require extensive quantitative knowledge on the magnetic properties of the particles. However, a large number of rising applications do require a careful magnetic characterization of these particles. Magnetic particles are, for example, used as magnetic labels for detection of target molecules in magnetic biosensors,[2,3] for microfluidic applications in lab-on-a-chip systems,[4] for characterization of the mechanical properties of cells,[5] or for measuring biological binding forces.[6] For many applications, nanometer sized particles are becoming increasingly important because of their minimum interference with biological processes.[7]

The properties of magnetic particles depend on a variety of factors, such as type and amount of magnetic material, the shape of the particle, and the microstructure. These factors can give rise to strong differences between individual magnetic particles. Therefore, magnetic characterization requires an individual particle approach. For micrometer sized magnetic particles such a technique exists in the form of magnetophoretic analysis.[8] However, for particles smaller than 1 μm, Brownian motion interferes with the measurements causing large measurement inaccuracies and problems with optical visibility.[9]

In this letter we describe a technique that breaks this 1 μm barrier by exploiting precisely the Brownian motion. The particle susceptibility can be calculated by analyzing the confined Brownian motion of the particle when trapped in a known magnetic potential well. Brownian motion analysis is commonly used in optical tweezers studies,[10] and occasionally in magnetic studies,[11–13] but it has not yet been used to characterize the magnetic properties of individual nanoparticles.

We defined a magnetic potential well on a chip by an integrated square current wire (see Fig. 1), suitable for trapping particle sizes down to 100 nm. For our first experiments we used superparamagnetic beads (Ademtech) with an average diameter of 300 nm, suspended in water. The chip sur-

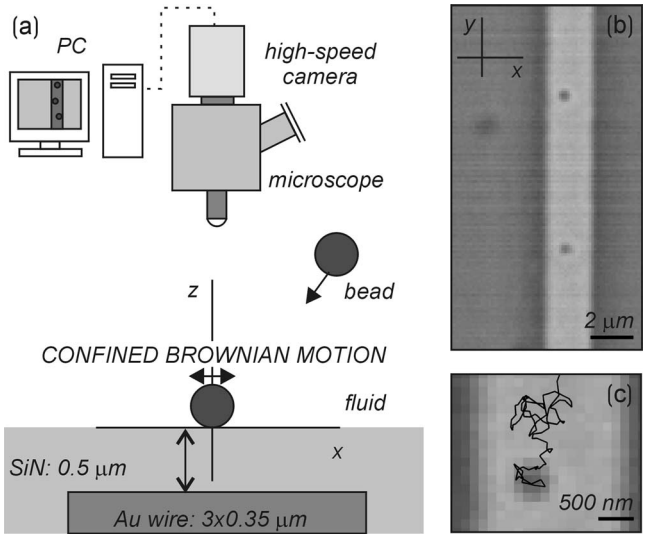

FIG. 1. (a) A Diluted suspension of 300 nm superparamagnetic beads (Ademtech) in water (10^8 beads/ml) is put on the chip surface. The superparamagnetic beads can be trapped in the magnetic potential well defined by a square gold current wire (3×0.35 μm^2) buried in a 0.5 μm layer of silicon nitride. In the x direction the Brownian motion is confined. In the y direction the bead is free to move. Movement in the z direction can be neglected, because the potential well is very steep in this direction. (b) The movement of the beads on the wire is observed with a microscope (Leica) with 160× water-immersion objective and a high-speed camera (MotionPro from Redlake, 250 fps). The pixel size is 125 nm. (c) Particle tracking software is used to resolve the trajectory of a bead with subpixel resolution.

[a]Electronic mail: kim.van.ommering@philips.com

face is examined with a high magnification optical microscope (160× water-immersion objective), and the movement of the beads is recorded with a high-speed camera (250 fps). The pixel size in a movie is 125 nm. The recorded movies are analyzed with particle tracking software to resolve the trajectories of the individual beads with subpixel resolution (40 nm).

A current through the wire generates a magnetic field that magnetizes the beads and attracts them to the wire. The magnetic potential energy U of the bead in the magnetic field can be calculated by taking the integral of the magnetization $\mathbf{M}$ and the magnetic field in the absence of the bead $\mathbf{B}$ over the bead volume V $\left(U=\int\frac{1}{2}\mathbf{M}\cdot\mathbf{B}dV\right)$.[14] For fields far below saturation, the change in magnetization as function of the field is defined as the volume susceptibility χ_v ($\mathbf{M}=\chi_v\mathbf{B}/\mu_0$). This volume susceptibility is a bead material property and includes demagnetization effects. We assume that the bead is surrounded by a nonmagnetic medium and that the field is constant over the volume of the bead. The resulting expression for the magnetic potential energy of the bead is then

$$U=\chi_v V\frac{\mathbf{B}^2}{2\mu_0}=\chi_{\text{bead}}\frac{\mathbf{B}^2}{2\mu_0}\quad\text{with}\quad\chi_{\text{bead}}=\chi_v V. \tag{1}$$

In the last equality we replaced the volume susceptibility χ_v by the bead susceptibility χ_{bead}.

The magnetic field around the current wire is calculated analytically using the law of Biot-Savart. The resulting expression is of the form $\mathbf{B}(\mathbf{x},\mathbf{y},\mathbf{z})=\mu_0\cdot(I/A)\cdot\mathbf{f}(\mathbf{x},\mathbf{y},\mathbf{z})$, with I the current, A the cross-sectional area of the wire, and $f(x,y,z)$ an analytical function that accounts for the geometry of the system. The magnetic field has a maximum above the center of the wire. At this point the bead is caught in a two-dimensional magnetic potential well: in the x direction and z direction the Brownian motion of the bead is confined, but in the y direction the bead is free to move. The movement of a trapped Brownian particle in equilibrium with its surroundings can be described by a Boltzmann distribution, including the magnetic energy and the thermal energy k_BT:[10,12]

$$P(x,z)\propto\exp\left(\frac{\chi_{\text{bead}}I^2(\mu_0\mathbf{f}(\mathbf{x},\mathbf{z})^2/2A^2)}{k_BT}\right). \tag{2}$$

Because this distribution function depends on the bead susceptibility, measuring the distribution of bead positions on the wire is a way to calculate the bead susceptibility. Clearly, Eq. (2) does not depend on friction forces, such as viscous drag or friction with the chip surface. These friction forces affect the kinetics of bead movement, but do not affect the distribution function in a potential well. Practically, this means that a susceptibility can be derived provided that the observation time is long enough ($t\gg w^2/D$, with w the width of the potential well and D the diffusion coefficient). Note that other techniques such as magnetophoresis do depend on viscous drag and therefore on the hydrodynamic radius of the bead.

In the experiments, individual beads are followed through a series of decreasing currents. Induced magnetic fields are around 5 mT, which is considerably lower than the saturation field of the beads (around 200 mT); therefore Eq. (1) is indeed valid. We estimated the Joule heating in the wires to be less than 10°C. In the current range used, we can neglect the movement in the z direction, because in this direction the potential well is steep compared to the x direction ($\nabla\mathbf{B}_z^2/\nabla\mathbf{B}_x^2>10$). The theoretical potential well and distribution function in the x direction for several currents and susceptibilities are shown in Fig. 2(a). For each measured current, a histogram of the bead positions is plotted and the theoretical probability function is fitted through the data, resulting in a susceptibility value [see Fig. 2(b)]. For broad distributions the error in the susceptibility is determined by the fit. For narrow distributions, the maximum accuracy is limited by the camera resolution and pixel size. The inset of Fig. 2(b) shows the measured susceptibilities of a few beads as function of the current. The measured values are on the order of the value we estimated from vibrating sample magnetometer measurements on bulk samples ($\chi_{\text{bead}}=0.4\times10^{-19}$ m^3). In some cases the susceptibility as function of the current is not constant. We have seen that this is usually nonreproducible, and therefore probably due to statistical fluctuations. We hypothesize that temporary sticking of beads to the surface plays an important role in this process.

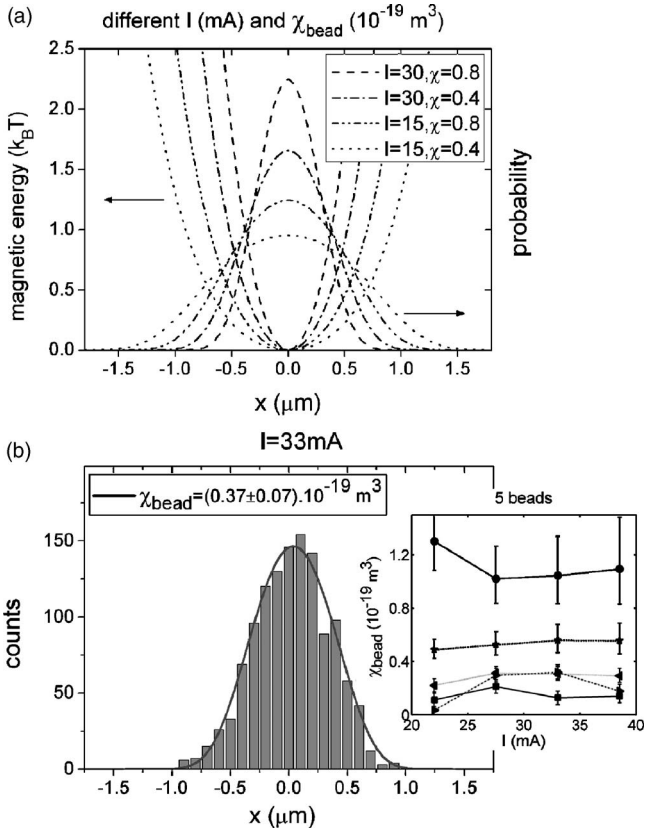

FIG. 2. (a) The theoretical magnetic potential well and distribution function are plotted for different currents I and susceptibilities χ_{bead}. (b) In the experiments individual beads are followed through a series of decreasing currents from 39 to 17 mA, in five steps of each 5 s. For each current a histogram of the bead position is made, using a bar size of 100 nm. The probability function is fitted through the data, resulting in a susceptibility value. The inset shows the calculated susceptibilities as function of the current for a few beads. Distinct differences between beads are observed.

We have observed distinct differences in susceptibility between beads from a single batch, going up to a factor of 10. An explanation for this large range in susceptibilities can be the difference in bead volume: for equal bead compositions and therefore equal χ_v, χ_{bead} is proportional to the volume. In transmission electron microscopy (TEM) images of the beads we observe bead diameters ranging from

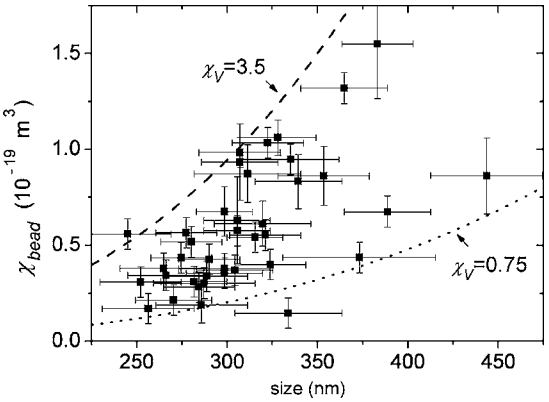

FIG. 3. The bead size is determined by fitting a two-dimensional Gaussian distribution through their intensity distribution in each movie frame. The susceptibility is calculated by taking the average of the value measured at a current of 33 mA and at a current of 28 mA. This graph shows that larger beads usually have a larger susceptibility. However, it is also clear that beads of the same size can have susceptibilities that differ more than a factor of 2; the volumetric susceptibility χ_v can thus differ between beads. The dashed lines represent curves of $\chi_{\text{bead}}=\chi_v\frac{1}{6}\pi d^3$, with d the estimated bead size.

150 to 450 nm, giving a volume variation of more than an order of magnitude. To examine the relation between susceptibility and size, we estimated the bead sizes in the movies by fitting a two-dimensional Gaussian distribution through their intensity distribution in each movie frame and correcting the found sizes for broadening due to diffraction. This gives an indication of their size with an estimated accuracy of 25 nm. The susceptibilities of 40 beads are plotted against their size in Fig. 3. This figure shows that larger beads usually have a larger susceptibility. However, it is also clear that beads of the same size can have susceptibilities that differ more than a factor of 2; χ_v can thus differ between beads. TEM images of the beads do not indicate large differences in the amount of magnetic material in beads with the same outer diameter; therefore also other factors such as grain sizes, distribution of magnetic material in the bead, or shape anisotropy might play a role.

Our next step will be to improve our setup to be able to obtain better statistical results in the analysis. Bead-surface interaction, such as temporary sticking, can be investigated by using different buffer fluids and surface chemistries. Measuring for longer times will minimize the influence of disturbances, but can be difficult because of an increasing bead concentration on the wire, which leads to undesired bead-bead interactions. However, our setup can be adapted by, for example, using a lower bead concentration and a preactuation step to collect beads on the surface or by using additional current wires to pull away the excess of beads on the wire. We will also study possible systematic errors, such as the assumption of a uniform field inside the beads, and the possibility of deviating dimensions of the current wires or isolating layer due to fabrication errors.

To conclude, we have described a technique that uses confined Brownian motion of individual nanoparticles on a chip to characterize their magnetic properties. Susceptibility measurements have been performed on 150–450 nm superparamagnetic beads. We found differences in bead susceptibility of an order of magnitude and differences in volumetric susceptibility of more than a factor of 2. Our technique can be used to find appropriate particles for applications or to examine the results of separation techniques. It is especially interesting that we can measure the susceptibility independent of the fluid viscosity and hydrodynamic radius of the bead, so the effect of these parameters in magnetophoretic separation techniques can be examined. Finally, we think that this technique does not just offer a way to determine the susceptibility of nanoparticles but that it opens another area of research. Our setup with the two-dimensional potential well offers the possibility to simultaneously analyze the distribution function of confined Brownian motion and the kinetics of free Brownian motion on a surface and is therefore a way to investigate general bead kinetics on chip surfaces. Also, it can be used to examine, for example, bead-bead interactions or bead-surface interactions. These factors are becoming increasingly important in microfluidic and lab-on-a-chip systems.

[1] Q. A. Pankhurst, J. Conolly, S. K. Jones, and J. Dobson, J. Phys. D **36**, R167 (2003).
[2] D. L. Graham, H. A. Ferreira, and P. P. Freitas, Trends Biotechnol. **22**, 455 (2004).
[3] M. Megens and M. Prins, J. Magn. Magn. Mater. **293**, 702 (2005).
[4] A. M. Gijs, Microfluid. Nanofluid. **1**, 22 (2004).
[5] B. G. Hosu, K. Jakab, P. Bánki, F. I. Tóth, and G. Forgacs, Rev. Sci. Instrum. **74**, 4158 (2003).
[6] M. Panhorst, P. Kamp, G. Reiss, and H. Brückl, Biosens. Bioelectron. **20**, 1685 (2005).
[7] J. P. Hancock and J. T. Kemshead, J. Immunol. Methods **164**, 51 (1993).
[8] S. Reddy, L. R. Moore, L. Sun, M. Zborowski, and J. J. Chalmers, Chem. Eng. Sci. **51**, 947 (1996).
[9] U. O. Häfeli, M. A. Lobedann, J. Steingroewer, L. R. Moore, and J. Riffle, J. Magn. Magn. Mater. **293**, 224 (2005).
[10] K. C. Neuman and S. M. Block, Rev. Sci. Instrum. **75**, 2787 (2004).
[11] E. Mirowksi, J. Moreland, S. E. Russek, and M. J. Donahue, Appl. Phys. Lett. **84**, 1786 (2004).
[12] L. E. Helseth, H. Z. Wen, P. Heinig, and Th M. Fischer, Langmuir **20**, 6556 (2004).
[13] C. Gosse and V. Croquette, Biophys. J. **82**, 3314 (2002).
[14] J. D. Jackson, *Classical Electrodynamics*, 3rd ed. (Wiley, New York, 1999).